Progress In Electromagnetics Research, PIER 23, 221–237, 1999

EFFECTS OF SURFACE HELICAL CONDUCTANCES ON MULTIPLE INTERACTIONS OF COMPOSITE ECCENTRICALLY BIANISOTROPIC CYLINDERS: THE CASE OF TM_z-WAVE INCIDENCE

W.-Y. Yin and L.-W. Li

Department of Electrical Engineering
National University of Singapore
10 Kent Ridge Crescent
Singapore 119260

1. INTRODUCTION

It is well known that scattering of electromagnetic waves by various cylindrical objects has long been studied by many people, and these studies have been motivated both by scientific interests in developing new techniques for solving scattering problems and by numerous engineering applications. More recently, Korshunova, Sivov, Shatrov, *et al.* have investigated the interaction of electromagnetic waves with cylindrical objects but possessing perfect electric or magnetic conductance along helical lines, and some novel phenomena have been demonstrated as well as practical applications in electromagnetic engineering have been proposed [1–5]. On the other hand, Kishk and Kildal have also examined the scattering from a dielectric cylinder with T- and L-strips using both theoretical and experimental methods [6]. It is apparently seen that the electromagnetic scattering from cylindrical bianisotropic objects has been investigated in [7–9] while the related models have also been examined in the previous studies [10–13]. To the authors' best knowledge, no work has, however, been done concerning with the scattering effect resulted from the helical conductance on the surface of inhomogeneous bianisotropic cylinder.

In this contribution, the authors pay attention to the effects of the helical conductance of the surface on the multiple scattering characteristics of impedance cylinders eccentrically coated with bianisotropic media. In the investigations, the T- and L-strips can be regarded as the special cases of the helical conductance of the cylindrical surface, and are thus used to examine the applicability of the technique proposed in this paper and the correctness of the results presented. The methodologies combined and employed in the theoretical analysis are the boundary-value technique and the method of generalized separation variables.

2. DESCRIPTION OF THE PROBLEM

Fig. 1(a) presents the geometry of the problem, in which N parallel, infinitely long, non-overlapping anisotropic impedance cylinders eccentrically coated with bianisotropic media are embedded in an isotropic medium (ε_b, μ_b). The cross section of the qth composite cylinder is shown in Fig. 1(b), and its radii are respectively denoted by $R_1^{(q)}$ and $R_2^{(q)}$, while the eccentric distance stands for $d^{(q)}(q = 1, 2, \cdots, N)$. In the host coordinate system (X, Y, Z), the location of the qth cylinder is noted by (ρ'_q, φ'_q), and the incident plane wave is in the direction of $\overline{k}(k_b, \theta_0, \varphi_0) = k_b(\sin\theta_0 \cos\varphi_0 \overline{e}_x + \sin\theta_0 \sin\varphi_0 \overline{e}_y + \cos\theta_0 \overline{e}_z)$, here $(\overline{e}_x, \overline{e}_y, \overline{e}_z)$ are the three unit vectors in the host coordinate system.

In the analysis, the constitutive features of the bianisotropic coating are described by the linear equations as $(e^{j\omega t})$:

$$\vec{D}^{(q)} = \left[\varepsilon^{(q)}\right] \vec{E}^{(q)} + \left[\xi_e^{(q)}\right] \vec{H}^{(q)} \tag{1a}$$

$$\vec{B}^{(q)} = \left[\mu^{(q)}\right] \vec{H}^{(q)} + \left[\xi_m^{(q)}\right] \vec{E}^{(q)} \tag{1b}$$

where $\left[\varepsilon^{(q)}\right]$, $\left[\mu^{(q)}\right]$, $\left[\xi_e^{(q)}\right]$, and $\left[\xi_m^{(q)}\right]$ are the permittivity tensor, permeability tensor, and magnetoelectric cross coupling tensors, respectively. In the cylindrical coordinate system the four constitutive

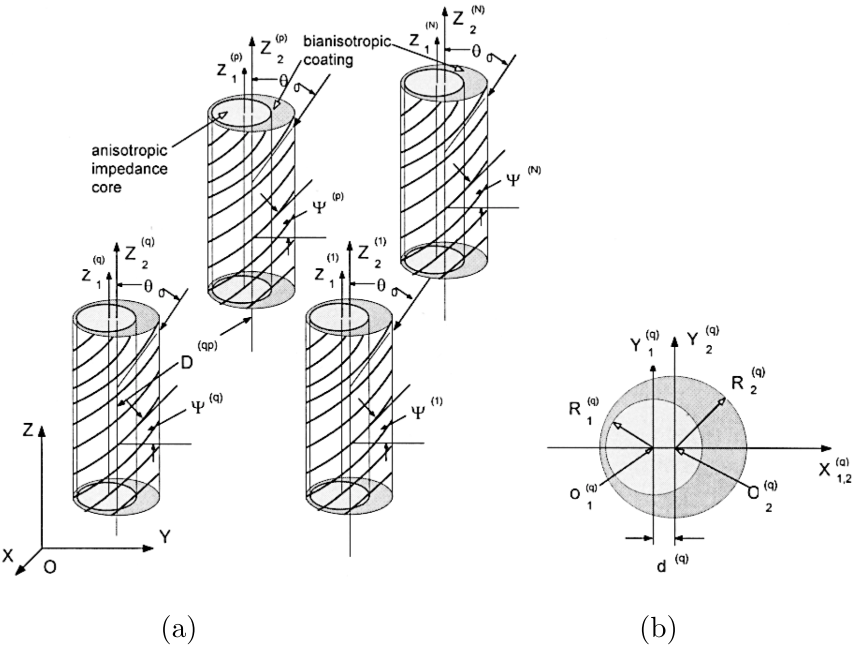

Figure 1. Geometry and coordinates of the N-parallel composite eccentric bianisotropic cylinders with the helical conductance at $\rho_2^{(q)} = R_2^{(q)}$. The separation between the adjacent cylinders $C^{(p)}$ and $C^{(q)}$ is noted by the distance $D^{(qp)}$ where $D^{(qp)} \geq (R_2^{(p)} + R_2^{(q)})$.

tensors, $O_2^{(q)}(\rho_2^{(q)}, \varphi_2^{(q)}, z_2^{(q)})\,(\rho_1^{(q)} \geq R_1^{(q)}, \rho_2^{(q)} \leq R_2^{(q)})$, are stated as

$$\left[C^{(q)}\right] = \begin{bmatrix} C_1^{(q)} & -jC_{12}^{(q)} & 0 \\ jC_{12}^{(q)} & C_1^{(q)} & 0 \\ 0 & 0 & C_2^{(q)} \end{bmatrix}, \quad C = \varepsilon,\ \mu,\ \xi_e,\ \xi_m\,. \tag{2}$$

In Fig. 1(a), the twist angle of helical line on the outer surface $\rho_2^{(q)} = R_2^{(q)}$ of bianisotropic coating is assumed to be $\Psi^{(q)}$. When $0 < \Psi^{(q)} < \frac{\pi}{2}$, the helical line is the right-handed, while $\frac{\pi}{2} < \Psi^{(q)} < \pi$ corresponds to the left-handed. Especially, when $\Psi^{(q)} = 0,\ \frac{\pi}{2}$ the helical surfaces are reduced to the T- and L-strips, respectively [6].

3. FIELD DISTRIBUTION

The excitation above is provided by a plane wave of TM_z-polarization with respect to the z-axis, and the incident electric and magnetic field components in the cylindrical coordinate system $O_2^{(q)}(\rho_2^{(q)}, \varphi_2^{(q)}, z_2^{(q)})$ are expressed as

$$E_{zinc}^{(q)} = E_0 \sin\theta_0 e^{jk_{b0}\rho'_q \cos(\varphi'_q - \varphi_0)} \sum_{n=-\infty}^{\infty} j^n J_{n2}^{(q)} e^{jn\left(\varphi_2^{(q)} - \varphi_0\right)} e_2^{(q)},$$
$$q = 1, 2, \cdots, N \tag{3a}$$

$$E_{\varphi inc}^{(q)} = E_0 \frac{\cos\theta_0}{k_{b0}\rho_2^{(q)}} e^{jk_{b0}\rho'_q \cos(\varphi'_q - \varphi_0)} \sum_{n=-\infty}^{\infty} j^n n J_{n2}^{(q)} e^{jn\left(\varphi_2^{(q)} - \varphi_0\right)} e_2^{(q)}, \tag{3b}$$

and

$$H_{\varphi inc}^{(q)} = -E_0 \frac{j\omega\varepsilon_b}{k_b} e^{jk_{b0}\rho'_q \cos(\varphi'_q - \varphi_0)} \sum_{n=-\infty}^{\infty} j^n J_{n2}^{(q)\prime} e^{jn\left(\varphi_2^{(q)} - \varphi_0\right)} e_2^{(q)}, \tag{3c}$$

where $J_{n2}^{(q)} = J_n(k_{b0}\rho_2^{(q)})$ is the nth-order Bessel function of the first kind, $J_{n2}^{(q)\prime} = J'_n(k_{b0}\rho_2^{(q)})$ denotes the derivative of $J_{n2}^{(q)}$ with respect to its argument, $k_{b0}^2 = k_b^2 - \beta^2$, $\beta = k_b \cos\theta_0$, $k_b = \omega\sqrt{\mu_b \varepsilon_b}$, and $e_2^{(q)} = e^{j\beta z_2^{(q)}}$.

Using the method of generalized separation variables and following the similar procedure adopted in [12], it is found that the tangential field components in the bianisotropic coating with respect to the coordinate system $O_2^{(q)}(\rho_2^{(q)}, \varphi_2^{(q)}, z_2^{(q)})$ can be expressed as

$$\begin{bmatrix} E_{z1}^{(q)} \\ H_{z1}^{(q)} \\ E_{\varphi 1}^{(q)} \\ H_{\varphi 1}^{(q)} \end{bmatrix} = \sum_{m=-\infty}^{\infty} \sum_{n=-\infty}^{\infty} \begin{bmatrix} V_{nm}^{(q,1)}(\rho_2^{(q)}) & V_{nm}^{(q,2)}(\rho_2^{(q)}) \\ V_{nm}^{(q,3)}(\rho_2^{(q)}) & V_{nm}^{(q,4)}(\rho_2^{(q)}) \\ V_{nm}^{(q,5)}(\rho_2^{(q)}) & V_{nm}^{(q,6)}(\rho_2^{(q)}) \\ V_{nm}^{(q,7)}(\rho_2^{(q)}) & V_{nm}^{(q,8)}(\rho_2^{(q)}) \end{bmatrix} e^{jn\varphi_2^{(q)}} \tag{4}$$

where $V_{nm}^{(q,s)}(\rho_2^{(q)})\,(s = 1, 2, \cdots, 8)$ are presented in [12] and suppressed here, however, it must be noted that here $\beta = k_b \cos\theta_0 \neq 0$. At the anisotropic impedance surface

$$\rho_1^{(q)} = R_1^{(q)}, \quad E_{z1}^{(q)} = -\eta_z^{(q)} H_{1\varphi}^{(q)}, \quad E_{\varphi 1}^{(q)} = \eta_\varphi^{(q)} H_{z1}^{(q)} \tag{5}$$

and when $\eta_z^{(q)} = \infty$, $\eta_\varphi^{(q)} = 0$, the impedance surface becomes soft, while $\eta_z^{(q)} = 0$, $\eta_\varphi^{(q)} = \infty$ corresponds to the hard surface [14, 15]. $D_{1n}^{(q)}$ and $D_{2n}^{(q)}$ in (4) are the unknown coefficients to be determined and the translational addition theorem for cylindrical wave functions has been employed in order to obtain the tangential field components in (4).

The total tangential field components outside the bianisotropic coating $(\rho_2^{(q)} \geq R_2^{(q)})$ can be written as the following form with respect to $O_2^{(q)}(\rho_2^{(q)}, \varphi_2^{(q)}, z_2^{(q)})$,

$$E_{z2}^{(q)} = E_{zinc}^{(q)} + \sum_{n=-\infty}^{\infty} a_n^{(q)} H_{n2}^{(q)} e_{\varphi 2}^{(q)} e_2^{(q)} + \sum_{\substack{l=1\\ l\neq q}}^{N} \sum_{n=-\infty}^{\infty} a_n^{(l)} H_{n2}^{(l)} e_{\varphi 2}^{(l)} e_2^{(l)} \tag{6a}$$

$$H_{z2}^{(q)} = \sum_{n=-\infty}^{\infty} b_n^{(q)} H_{n2}^{(q)} e_{\varphi 2}^{(q)} e_2^{(q)} + \sum_{\substack{l=1\\ l\neq q}}^{N} \sum_{n=-\infty}^{\infty} b_n^{(l)} H_{n2}^{(l)} e_{\varphi 2}^{(l)} e_2^{(l)} \tag{6b}$$

$$\begin{aligned} E_{\varphi 2}^{(q)} = E_{\varphi inc}^{(q)} &+ \frac{\cos\theta_0}{k_b \sin^2\theta_0} \\ &\cdot \left[\sum_{n=-\infty}^{\infty} a_n^{(q)} \frac{n}{\rho_2^{(q)}} H_{n2}^{(q)} e_{\varphi 2}^{(q)} e_2^{(q)} + \sum_{\substack{l=1\\ l\neq q}}^{N} \sum_{n=-\infty}^{\infty} a_n^{(l)} \frac{n}{\rho_2^{(l)}} H_{n2}^{(l)} e_{\varphi 2}^{(l)} e_2^{(l)} \right] \\ &+ \frac{j\omega\mu_b}{k_{b0}} \left[\sum_{n=-\infty}^{\infty} b_n^{(q)} H_{n2}^{(q)\prime} e_{\varphi 2}^{(q)} e_2^{(q)} + \sum_{\substack{l=1\\ l\neq q}}^{N} \sum_{n=-\infty}^{\infty} b_n^{(l)} H_{n2}^{(l)\prime} e_{\varphi 2}^{(l)} e_2^{(l)} \right] \end{aligned} \tag{6c}$$

$$H_{\varphi 2}^{(q)} = H_{\varphi inc}^{(q)} - \frac{j\omega\varepsilon_b}{k_{b0}} \left[\sum_{n=-\infty}^{\infty} a_n^{(q)} H_{n2}^{(q)'} e_{\varphi 2}^{(q)} e_2^{(q)} + \sum_{\substack{l=1 \\ l\neq q}}^{N} \sum_{n=-\infty}^{\infty} a_n^{(l)} H_{n2}^{(l)'} e_{\varphi 2}^{(l)} e_2^{(l)} \right] + \frac{\cos\theta_0}{k_b \sin^2\theta_0} \left[\sum_{n=-\infty}^{\infty} b_n^{(q)} \frac{n}{\rho_2^{(q)}} H_{n2}^{(q)} e_{\varphi 2}^{(q)} e_2^{(q)} + \sum_{\substack{l=1 \\ l\neq q}}^{N} \sum_{n=-\infty}^{\infty} b_n^{(l)} \frac{n}{\rho_2^{(l)}} H_{n2}^{(l)} e_{\varphi 2}^{(l)} e_2^{(l)} \right] \tag{6d}$$

where $H_{n2}^{(q)} = H_n^{(2)}(k_{b0}\rho_2^{(q)})$ is the nth-order Hankel function of the second kind, $H_{n2}^{(q)'} = H_n^{(2)'}(k_{b0}\rho_2^{(q)})$ denotes the derivative of $H_{n2}^{(q)}$ with respect to its argument, $e_{\varphi 2}^{(q)} = e^{jn\varphi_2^{(q)}}$, and $a(b)_n^{(q)} (q = 1, 2, \cdots, N)$ are the unknown scattering coefficients.

The approximate boundary conditions for the helical conductance on the surface $\rho_2^{(q)} = R_2^{(q)}$ are

$$\begin{aligned} &E_{z1}^{(q)} = E_{z2}^{(q)}, \quad E_{\varphi 1}^{(q)} = E_{\varphi 2}^{(q)}, \quad E_{\varphi 1}^{(q)} + E_{z1}^{(q)} \tan\Psi^{(q)} = 0, \\ &H_{\varphi 1}^{(q)} + H_{z1}^{(q)} \tan\Psi^{(q)} = H_{\varphi 2}^{(q)} + H_{z2}^{(q)} \tan\Psi^{(q)}. \end{aligned} \tag{7a}$$

For the eccentric bianisotropic coating with T-strips $(\Psi^{(q)} = 0)$, we have

$$E_{z1}^{(q)} = E_{z2}^{(q)}, \quad E_{\varphi 1}^{(q)} = E_{\varphi 2}^{(q)} = 0, \quad H_{\varphi 1}^{(q)} = H_{\varphi 2}^{(q)}. \tag{7b}$$

while for L-strips $(\Psi^{(q)} = 90°)$, we get

$$E_{z1}^{(q)} = E_{z2}^{(q)} = 0, \quad E_{\varphi 1}^{(q)} = E_{\varphi 2}^{(q)}, \quad H_{z1}^{(q)} = H_{z2}^{(q)}. \tag{7c}$$

To enforce the above boundary conditions at $\rho_2^{(q)} = R_2^{(q)}$ to be satisfied, the translational addition theorem for the cylindrical Hankel function, $H_{n2}^{(l)}$, should be employed, i.e.,

$$H_n^{(2)}\left(k_{b0}\rho_2^{(l)}\right) e^{in\varphi_2^{(l)}} = \sum_{m=-\infty}^{+\infty} H_{m-n}^{(2)}\left(k_{b0}D_{ql}\right) J_m\left(k_{b0}\rho_2^{(q)}\right) e^{i\left[m\varphi_2^{(q)} - (m-n)\varphi_{ql}\right]} \tag{8a}$$

and

$$D_{ql}^2 = {\rho'_q}^2 + {\rho'_l}^2 - 2\rho'_q\rho'_l \cos\left(\varphi'_q - \varphi'_l\right) \tag{8b}$$

$$\varphi_{ql} = \begin{cases} \cos^{-1}\left(\dfrac{\rho'_q \cos\varphi'_q - \rho'_l \cos\varphi'_l}{D_{ql}}\right), & \rho'_q \sin\varphi'_q \geq \rho'_l \sin\varphi'_l, \\ -\cos^{-1}\left(\dfrac{\rho'_q \cos\varphi'_q - \rho'_l \cos\varphi'_l}{D_{ql}}\right), & \rho'_q \sin\varphi'_q < \rho'_l \sin\varphi'_l. \end{cases} \tag{8c}$$

Finally, N sets of equation for N cylinders can be derived for determining the unknown scattering coefficients $a(b)_n^{(q)}(q = 1, 2, \cdots, N)$ and the tedious mathematical manipulations are suppressed here. Therefore, by using the large argument approximation of the Hankel function, both the co- and the cross-polarized scattering cross sections of the above multiple cylinders can be calculated by

$$\sigma^{co}(\varphi) = \frac{4}{k_b \sin^4\theta_0 |E_0|^2} \left| \sum_{q=1}^{N} e^{jk_{b0}\cos(\varphi'_q - \varphi)} \sum_{n=-\infty}^{\infty} a_n^{(q)} j^n e^{jn\varphi} \right| \tag{9a}$$

$$\sigma^{cross}(\varphi) = \frac{4\omega^2\mu_b^2}{k_b^3 \sin^4\theta_0 |E_0|^2} \left| \sum_{q=1}^{N} e^{jk_{b0}\cos(\varphi'_q - \varphi)} \sum_{n=-\infty}^{\infty} b_n^{(q)} j^n e^{jn\varphi} \right|. \tag{9b}$$

For the case of TE$_z$-wave obliquely incidence, $\sigma^{co(cross)}(\varphi)$ can also be calculated by following the similar way as above.

4. NUMERICAL RESULTS AND DISCUSSION

Of particular interest here are the effects of the helical conductance of the surface on the co- and cross-polarized scattering cross sections of the composite, eccentric bianisotropic cylinder array. Therefore some computer codes have been developed for calculating the $\sigma^{co,cross}$ for the TM$_z$-wave obliquely incidence. For practical consideration, in the following numerical examples we let $\varepsilon_b = \varepsilon_0$ and $\mu_b = \mu_0$.

At first, Fig. 2 depicts the $\sigma^{co(cross)}$ as a function of φ for the case of four composite bianisotropic cylinders corresponding to different twist angles $\psi^{(q)}(q = 1, 2, 3, 4)$, respectively.

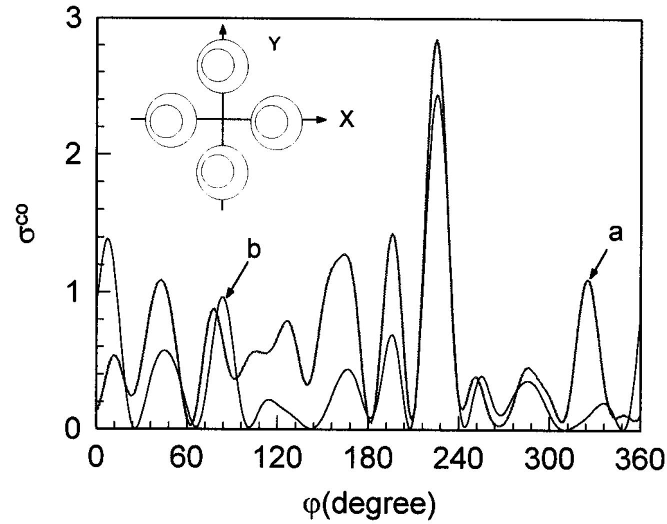

3
2
1
0
σ^co
Y
X
a
b
0 60 120 180 240 300 360
φ(degree)

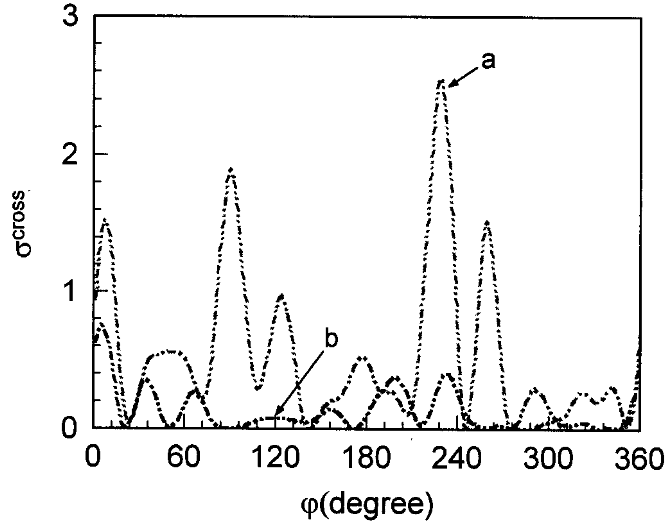

3
2
1
0
σ^cross
a
b
0 60 120 180 240 300 360
φ(degree)

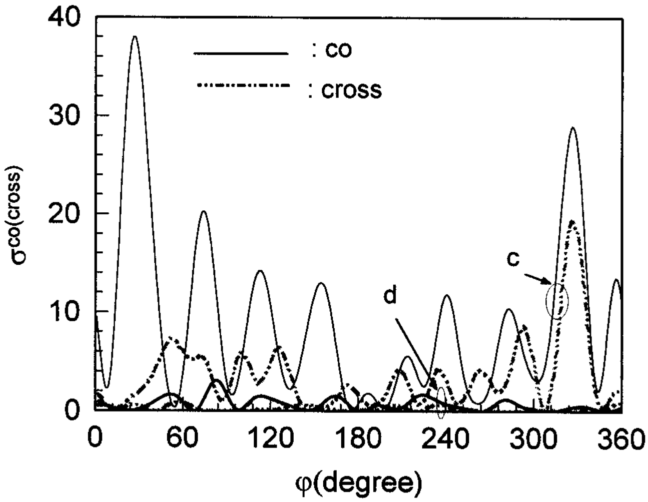

Figure 2. $\sigma^{co(cross)}$ versus φ for four bianisotropic eccentric cylinders possessing helical conductance of the surface. $f = 10\,\text{GHz}$, $N_0 \geq 8$, $E_0 = 1$,
$k_b\rho'_q = 10.0$, $\varphi'_q = 0°$, $90°$, $180°$, $270°$, $k_bR_1^{(q)} = 1.0$, $k_bR_2^{(q)} = 2.0$,
$\eta_z^{(q)} = \eta_\varphi^{(q)} = 0.5(1.0 - j1.0)\eta_0$, $\mu_2^{(q)} = \mu_0$, $\mu_1^{(q)} = \mu_0\omega_0^{(q)}\omega_m^{(q)} / \left[{\omega_0^{(q)}}^2 - \omega^2\right]$,
$\mu_{12}^{(q)} = -\mu_0\omega\omega_m^{(q)} / \left[{\omega_0^{(q)}}^2 - \omega^2\right]$, $M_s^{(q)}\mu_0 = 0.16T$, $\omega_m^{(q)} = 2.21 \times 10^5 M_s^{(q)}$,
$\omega_0^{(q)}/\omega_m^{(q)} = 0.3$, $q = 1, 2, 3, 4$,

$$\left[\varepsilon^{(q)}\right] = \varepsilon_0 \begin{bmatrix} 4.0 & -j0.5 & 0 \\ j0.5 & 4.0 & 0 \\ 0 & 0 & 4.5 \end{bmatrix},$$

$$\left[\xi_e^{(q)}\right] = -\left[\xi_m^{(q)}\right] = \sqrt{\mu_0\varepsilon_0} \begin{bmatrix} j0.5 & -j0.3 & 0 \\ j0.3 & j0.5 & 0 \\ 0 & 0 & j0.6 \end{bmatrix} (D_\infty)(C_\infty)).$$

(a) $k_bd^{(q)} = 0.5$, $\varphi_0 = \theta_0 = 45°$, $\psi^{(q)} = 30°$;
(b) $k_bd^{(q)} = 0.5$, $\varphi_0 = \theta_0 = 45°$, $\psi^{(q)} = 60°$;
(c) $k_bd^{(q)} = 0.5$, $\varphi_0 = \theta_0 = \psi^{(q)} = 45°$;
(d) $k_bd^{(q)} = 0.0$, $\varphi_0 = \theta_0 = \psi^{(q)} = 45°$ (concentric case).

In Fig. 2, four composite cylinders are located at $k_b\rho'_q = 10.0$, and $\varphi'_q = 0°$, $90°$, $180°$, and $270°$, respectively. The bianisotropic coating is lossless and its four constitutive tensors is assumed to be in the form of the magnetic group of symmetry $D_\infty(C_\infty)$ [16]. It is clear that both σ^{co} and σ^{cross} are, generally speaking, strongly governed by the twist angle $\psi^{(q)}$. Especially for case (c), $\sigma^{co(cross)}$ are much larger than that of case (a) or (b), and nearly resonant scattering is expected under such circumstances. We know that at low-frequency the resonance phenomenon for a magnetodielectric rod with an anisotropic helical conductance of the surface has already been examined in [4]. Interestingly, for the concentric case (d), $\sigma^{co(cross)}$ are much lower than that of case (c), and the resonant scattering effect is disappear. Here, it should be pointed out that the convergence behavior of the truncation terms in the series summation has also been checked for above calculations, and Table 1 lists some values of $\sigma^{co(cross)}$ corresponding to cases (a) and (c), respectively. It is obvious that at lest five-digit accuracy can be achieved for $N_0 \geq 10$. On the other hand, if θ_0 approaches $0°$ or $180°$, more terms should be kept in the series summations.

M	(a)		(c)	
	σ^{co}	σ^{cross}	σ^{co}	σ^{cross}
2	3.62182	2.95561	57.22894	46.99395
3	2.90889	2.37656	31.39699	20.90939
4	2.84134	2.38254	28.87429	19.23102
5	2.84297	2.37451	28.97975	19.31200
6	2.84260	2.37440	28.96073	19.30056
7	2.84257	2.37435	28.95895	19.29959
8	2.84256	2.37435	28.95870	19.29945
9	2.84256	2.37435	28.95866	19.29942
10	2.84256	2.37435	28.95865	19.29942
11	2.84256	2.37435	28.95865	19.29942

Table 1. $\sigma^{co(cross)}$ against $N_0(m, n = -N_0, \cdots, N_0)$ for cases (a) $(\varphi = 225°)$ and (c) $(\varphi = 327°)$.

Fig. 3 shows the co- and cross-polarized scattering characteristics of four composite uniaxal bianisotropic cylinders $(\sigma^{co(cross)} \geq 0)$, and the twist angle is chosen to be in different values.

In Fig. 3, the four constitutive tensors of the uniaxial bianisotropic coating are in the form of the magnetic group D_∞. For curve (a) we chose $\varphi_0 = \theta_0 = \psi^{(q)} = 45°$, while curve (b) stands for the normally incident case $(\theta_0 = 90°)$. Under such conditions, the magnitude of σ^{cross} is much lower than that of curve (a) and even for the co-polarized component. Comparing curve (c) with (d), it is clear that the cross-polarized scattering effect is not enhanced for curve (d) even if we let $\varphi_0 = \theta_0 = \psi^{(q)} = 60°$. On the other hand, it should be noted that the above four cylinders possess double 'chiralities' or double helicals: one is presented by the cross-coupling tensors $\left[\xi_e^{(q)}\right]$ and $\left[\xi_m^{(q)}\right]$ of the uniaxial form $(\left[\xi_m^{(q)}\right] = -\left[\xi_e^{(q)}\right])$, and the other is resulted from the helical conductance of the surface described by the twist angle $\psi^{(q)}$. Various numerical experiments prove that, for symmetrical incidence $\varphi_0 = 0°(180°)$,

$$\begin{aligned}\sigma^{co(cross)}&\left(\theta_0, \psi^{(q)}, \left[\xi_e^{(q)}\right], \left[\xi_m^{(q)}\right]\right)\\ &= \sigma^{co(cross)}\left(180° - \theta_0, 180° - \psi^{(q)}, \left[\xi_m^{(q)}\right], \left[\xi_e^{(q)}\right]\right);\end{aligned} \tag{10a}$$

and for normally incidence $\theta_0 = 90°$,

$$\begin{aligned}\sigma^{co(cross)}&\left(\varphi_0, \psi^{(q)}, \left[\xi_e^{(q)}\right], \left[\xi_m^{(q)}\right]\right)\\ &= \sigma^{co(cross)}\left(-\varphi_0, 180° - \psi^{(q)}, \left[\xi_m^{(q)}\right], \left[\xi_e^{(q)}\right]\right);\end{aligned} \tag{10b}$$

where $\psi^{(q)} \to 180° - \psi^{(q)}$ and exchanging the position of $\left[\xi_e^{(q)}\right]$ and $\left[\xi_m^{(q)}\right]$ in (10) means that, physically, reverse the rotations of the double helicals simultaneously. (10) has no relation to the operating frequency, the geometrical size or location of each cylinder array, and it also holds true for the TE$_z$-wave incidence.

Furthermore, Fig. 4 depicts the $\sigma^{co,cross}$ as a function of φ for four composite uniaxal bianisotropic cylinders with T-strips $(\psi^{(q)} = 0°)$.

In Fig. 4, curve (a) is the obliquely incidence and curve (b) is just the normally incidence. It is noted that for curve (a), the cross-polarized

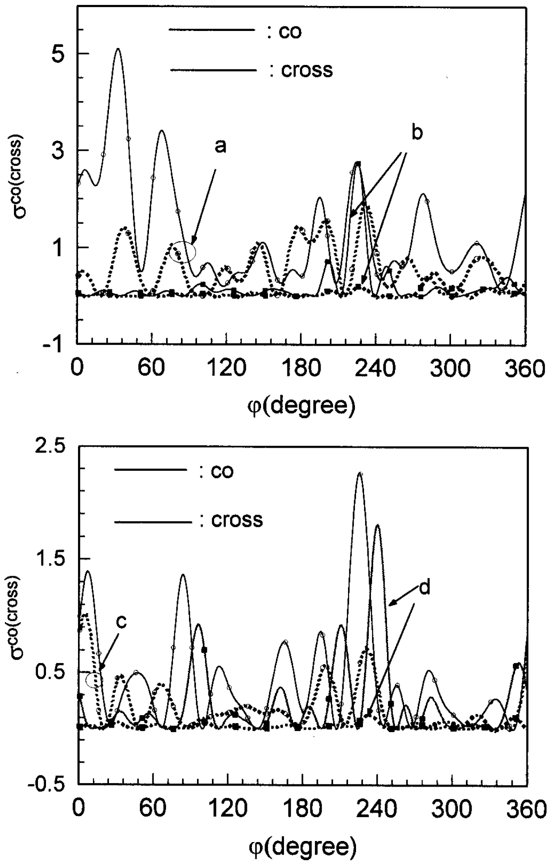

Figure 3. $\sigma^{co(cross)}$ versus φ for four uniaxial bianisotropic eccentric cylinders possessing helical conductance of the surface. The parameters are the same as Fig. 2, except that

$$\left[\varepsilon^{(q)}\right]=\varepsilon_0\begin{bmatrix}4.0&0&0\\0&4.0&0\\0&0&4.5\end{bmatrix},\quad \left[\mu^{(q)}\right]=\mu_0\begin{bmatrix}1.0&0&0\\0&1.0&0\\0&0&1.5\end{bmatrix},$$

$$\left[\xi_e^{(q)}\right]=-\left[\xi_m^{(q)}\right]=\sqrt{\mu_0\varepsilon_0}\begin{bmatrix}j0.6&0&0\\0&j0.6&0\\0&0&j0.8\end{bmatrix}(D_\infty),$$

(a) $\varphi_0=\theta_0=\psi^{(q)}=45^\circ$ (circular dot);
(b) $\theta_0=90^\circ,\ \varphi_0=\psi^{(q)}=45^\circ$ (square dot);
(c) $\varphi_0=\theta_0=45^\circ,\ \psi^{(q)}=60^\circ$ (circular dot);
(d) $\varphi_0=\theta_0=\psi^{(q)}=60^\circ$ (square dot).

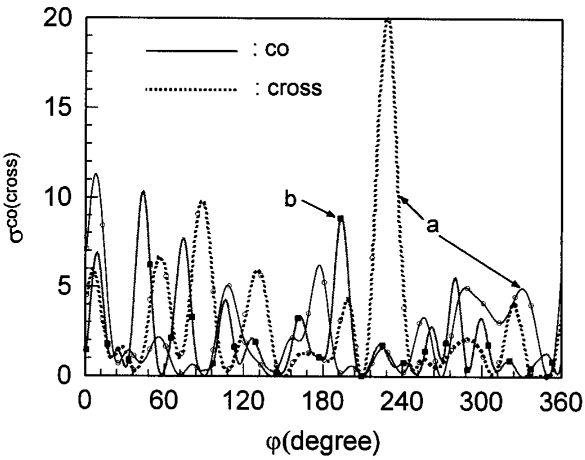

Figure 4. $\sigma^{co(cross)}$ versus φ for four uniaxial bianisotropic eccentric cylinders with T-strips. The parameters are the same as Fig. 3, except that (a) $\varphi_0 = \theta_0 = 45°$ (circular dot) and (b) $\theta_0 = 90°$, $\varphi_0 = 45°$ (square dot).

scattering effect is enhanced greatly and σ^{cross} reaches the maximum in the nearly forward direction $\varphi = 225°$. While for curve (b), since $\theta_0 = 90°$, no cross-polarized scattered field component can be expected for the T-strips case. Also, numerical experiments prove that:

$$\begin{aligned}\sigma^{co}&\left(\theta_0 = 90°, \varphi_0, \left[\xi_e^{(q)}\right], \left[\xi_m^{(q)}\right], \varphi\right)\\ &= \sigma^{co}\left(\theta_0 = 90°, -\varphi_0, \left[\xi_m^{(q)}\right], \left[\xi_e^{(q)}\right], 360° - \varphi\right)\end{aligned} \tag{11a}$$

$$\begin{aligned}\sigma^{co(cross)}&\left(\theta_0, \varphi_0 = 0°(180°), \left[\xi_e^{(q)}\right], \left[\xi_m^{(q)}\right]\right)\\ &= \sigma^{co(cross)}\left(180° - \theta_0, \varphi_0 = 0°(180°), \left[\xi_m^{(q)}\right], \left[\xi_e^{(q)}\right]\right).\end{aligned} \tag{11b}$$

The equation (11b) is also true for the magnetic group $D_\infty(C_\infty)$ (in Fig. 2).

Finally, Fig. 5 depicts the co- and cross-polarized scattering characteristics of four composite uniaxial bianisotropic cylinders with L-strips ($\psi^{(q)} = 90°$).

In Fig. 5, it is interesting to note that, for both constitutive models described by the magnetic groups D_∞ and $D_{\infty h}(C_{\infty\nu})$ [17], the co-polarized scattered field component is just the same for either

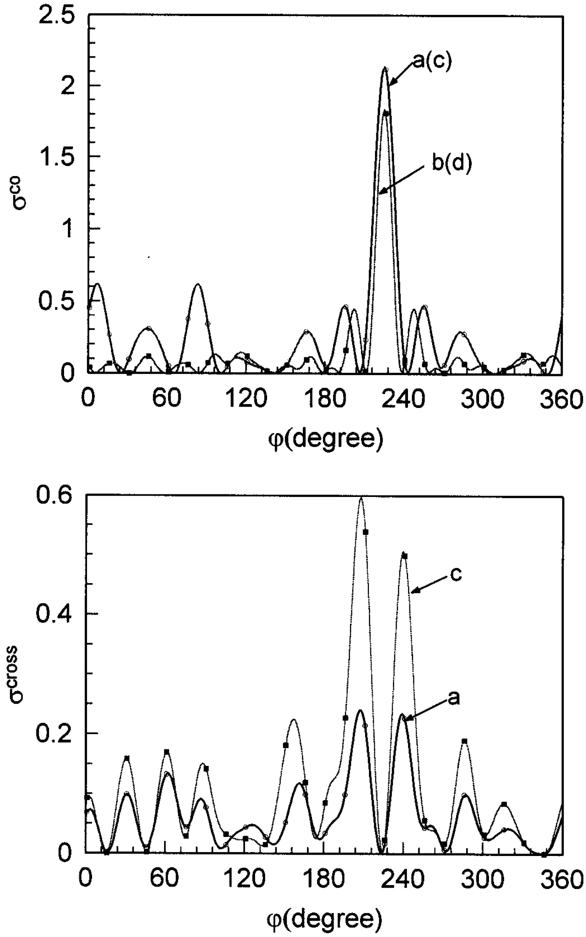

Figure 5. $\sigma^{co(cross)}$ versus φ for four uniaxial bianisotropic eccentric cylinders with L-strips. The parameters for (a) and (b) are the same as Fig. 4, i.e.,

for (a) (b): $\left[\xi_e^{(q)}\right] = -\left[\xi_m^{(q)}\right] = \sqrt{\mu_0\varepsilon_0}\begin{bmatrix} j0.6 & 0 & 0 \\ 0 & j0.6 & 0 \\ 0 & 0 & j0.8 \end{bmatrix}(D_\infty);$

for (c) (d): $\left[\xi_e^{(q)}\right] = -\left[\xi_m^{(q)}\right] = \sqrt{\mu_0\varepsilon_0}\begin{bmatrix} 0 & -j0.6 & 0 \\ j0.6 & 0 & 0 \\ 0 & 0 & 0 \end{bmatrix}(D_{\infty h}(C_{\infty\nu}));$

for (a) (c) $\varphi_0 = \theta_0 = 45°$; and

for (b) (d) $\theta_0 = 90°, \varphi_0 = 45°$.

$\varphi_0 = \theta_0 = 45°$ or $\theta_0 = 90°, \varphi_0 = 45°$. The main deference between D_∞ and $D_{\infty h}(C_{\infty\nu})$ is that the cross-polarized effect in the scattered field is different for obliquely incidence. Relatively speaking, for $D_{\infty h}(C_{\infty\nu})$ the magnitude of σ^{cross} is much higher than that of D_∞. Also, as the above T-strips case, σ^{cross} is zero for the L-strips for normally incidence, and $(\psi^{(q)} = 90°)$

$$\sigma^{co}\left(\theta_0, \varphi_0, \left[\xi_e^{(q)}\right], \left[\xi_m^{(q)}\right], \varphi\right) \tag{12a}$$
$$= \sigma^{co}\left(180° - \theta_0, -\varphi_0, \left[\xi_m^{(q)}\right], \left[\xi_e^{(q)}\right], 360° - \varphi\right)(D_\infty)$$
$$\sigma^{co(cross)}\left(\theta_0, \varphi_0, \left[\xi_e^{(q)}\right], \left[\xi_m^{(q)}\right], \varphi\right) \tag{12b}$$
$$= \sigma^{co(cross)}\left(180° - \theta_0, -\varphi_0, \left[\xi_m^{(q)}\right], \left[\xi_e^{(q)}\right], 360° - \varphi\right)\left[D_{\infty h}(C_{\infty\nu})\right].$$

5. CONCLUSION

In this study, our attention has been paid to the scattering from multiple composite bianisotropic cylinders possessing the right- and left-handed helical conductances of the surfaces, and some special information has been given about such unique structure. The above results show that, both the co- and the cross-polarized scattered cross sections of the scatterers are very sensitive to the twist angle, and its effect on the scattering of cylindrical objects is just diverse. For instance, under some circumstances, the resonant scattering phenomenon of the composite bianisotropic cylinders can be expected under the TM_z-wave incidence.

ACKNOWLEDGMENT

This work was supported with the funds by the National University of Singapore sponsored project RP3981676. W. Y. Yin also greatly appreciates the Alexander von Humboldt Foundation for sponsorship of his research in Germany.

REFERENCES

1. Korshunova, E. N., A. N. Sivov, and A. D. Shatrov, "Diffraction of plane circularly polarized waves by a grating made of circular cylinders with perfect surface electric and magnetic conductivities along the helical lines," *J. Commun. Tech. Electron.,* Vol. 41, No. 10, 847–850, 1996.
2. Stakanov, S. N. and A. I. Semenikhin, "Scattering of a plane wave by a cylinder with an anisotropic gyromagnetic twist- coating," *J. Commun. Tech. Electron.,* Vol. 41, No. 13, 1086–1093, 1996.
3. Zubov, A. S., A. N. Sivov, V. S. Solosin, A. D. Chuprin, and A. D. Shatrov, "Scattering of waves by cylinders with spiral surface conductivity and simulation of the electrodynamical characteristics of multi-link wire spirals with the help of such cylinders," *J. Commun. Tech. Electron.,* Vol. 41, No. 16, 1379–1382, 1996.
4. Pribytko, M. P. and A. D. Shatrov, "Low- frequency resonances in a magnetodielectric rod with an anisotropic helical conductance of the surface," *J. Commun. Tech. Electron.,* Vol. 42, No. 1, 17–21, 1997.
5. Korshunova, E. N., A. N. Sivov, and A. D. Shatrov, "Waves guided by a cylinder with perfect electric and magnetic conductances along helical lines," *J. Commun. Tech. Electron.,* Vol. 42, No. 1, 22–26, 1997.
6. Kishk, A. A. and P.-S. Kildal, "Asymptotic boundary conditions for strip-loaded scatterers applied to circular dielectric cylinders under oblique incidence," *IEEE Trans. Antennas and Propagat.,* Vol. AP-45, No. 1, 51–55, 1997.
7. Shen, Z. X., "Electromagnetic scattering by an impedance cylinder coated eccentrically with a chiroplasma," *IEE Proc.-Microw. Antennas Propagat.,* Vol. 141, No. 4, 279–284, 1994.
8. Jakoby, B., "Scattering of obliquely incident waves by an impedance cylinder with inhomogeneous bianisotropic coating," *IEEE Trans. Antennas Propagat.,* Vol. AP-45, No. 4, 648–655, 1997.
9. Cheng, D. J., Y. M. M. Antar, and G. Wang, "Electromagnetic scattering by a uniaxial chiral cylinder with arbitrary cross section: generalized mode-matching method," *Micro. Opt. Tech. Lett.,* Vol. 18, No. 6, 410–414, 1998.
10. Yin, W. Y., "Electromagnetic scattering by some composite bianisotropic eccentric cylinder," *Micro. Opt. Tech. Lett.,* Vol. 10, 177–182, 1995.
11. Yin, W. Y., "The features of Mueller scattering matrix for two penetrable composite Faraday chiral cylinders," *JEMWA,* Vol. 10, 1199–1216, 1996.

12. Yin, W. Y., H. L. Zhao, and W. Wan, "Parametric study on the scattering characteristics of two impedance cylinders eccentrically coated with Faraday chiral materials," *JEMWA,* Vol. 10, 1467–1484, 1996.
13. Yin, W. Y., "Scattering by a linear array of uniaxial bianisotropic chiral cylinders," *Micro. Opt. Tech. Lett.,* Vol. 12, No. 5, 287–295, 1996.
14. Kildal, P. S., "Artifically soft and hard surfaces in electromagnetics," *IEEE Trans. Antennas Propagat.,* Vol. AP-38, No. 10, 1537–1544, 1990.
15. Kildal, P. S., A. A. Kishk, and A. Tengs, "Reduction of forward scattering from cylindrical objects using hard surfaces," *IEEE Trans. Antennas Propagat.,* Vol. AP-44, 1509–1520, 1996.
16. Dmitriev, V., "Constitutive tensors and general properties of complex and bianisotropic media described by continuous groups of symmetry," *Electr. Lett.,* Vol. 34, No. 6, 532–534, 1998.
17. Dmitriev, V., "Degeneracy of dispersion equation eigenvalues of bianisotropic media and bidirectionality of these media," *Micro. Opt. Tech. Lett.,* Vol. 19, No. 3, 238–242, 1998.